Electronic structure of Be_2C

C. H. Lee,* W. R. L. Lambrecht, and B. Segall
Department of Physics, Case Western Reserve University, Cleveland, Ohio 44106-7079
(Received 6 September 1994)

The electronic band structure, lattice constant, bulk modulus, cohesive energy, complex dielectric function, and electron-energy-loss function for Be_2C are calculated by the linear-muffin-tin-orbital method. The calculated $-\mathrm{Im}(1/\epsilon)$ and partial densities of states are found to be in satisfactory accord, respectively, with the measured electron energy loss (EELS) in the low-loss region and with the K-shell electron-energy-loss-near-edge fine-structure measurements, the only available data relevant to the band structure. The band gap is found to be indirect (Γ-X) with a local-density-approximation value of 1.2 eV. The EELS data provide an estimate for the gap correction of ~ 2.0 eV.

I. INTRODUCTION

Interest in solids formed from atoms with low atomic numbers has recently increased greatly,[1] because of the potential unique properties of these materials. Some of these properties are associated with the relatively strong chemical bonding characteristic of the first row atoms, others with the frequent occurrence of large band gaps. The former leads to high melting points, which implies potential use as refractories and large elastic constants which, in turn, are related to hardness, high sound velocities and good thermal conductivities. The large band gaps could lead to potential interesting optical properties. Be_2C, which forms in the so-called antifluorite structure, has to date received relatively little attention. In part, this is due to the fact that this material tends to hydrolyze to $Be(OH)_2$ and to react with O and N. This study of the electronic structure of Be_2C is part of a larger theoretical effort to explore the nature and properties of low Z materials. In contrast to the previous subjects of inquiry, which had relatively strongly covalent character, Be_2C is apparently more strongly ionic. We also note that Be_2C has been found to occur in the epitaxial growth of diamond on BeO,[2,3] a subject of interest to us. It is also of interest as a possible starting material for the synthesis of $BeCN_2$.[4–6]

At present, there is very limited empirical data on the properties of this material in general and in the electronic properties in particular. The most relevant data for our purposes are those resulting from the electron-energy-loss studies on very small samples by Disko *et al.*[7] These studies can be divided into two groups: the first being the loss spectrum in the low-loss region (0 to about 50 eV), and the second being the higher-energy spectra associated with excitations of electrons from the Be and C K shells. The latter is referred to as K-shell electron-energy-loss near-edge fine structure (ELNES).

To our knowledge, there have been three previous calculations of the electronic structure of Be_2C. The first, by Herzig and Redinger (HR)[8], was a self-consistent augmented plane wave (APW) calculation. That calculation was carried out at the empirical lattice constant and thus did not investigate the "energetic" properties of the material. Also, this calculation employed the muffin-tin approximation, the validity of which for this material is open to question. (Note that 28% of the valence charge is found to be inside the "interstitial" region.)

The second was a simple semiempirical tight-binding calculation that accompanied the energy-loss measurements of Ref. 7. This approach is certainly limited by the paucity of relevant empirical data, as well as by the intrinsic limitations of such calculations. The same paper also contained a multiple scattering calculation of the ELNES spectra using a muffin-tin potential based on atomic potentials with a semiempirical adjustment for the charge transfer between Be and C.

The third calculation, by Corkill and Cohen (CC) (Ref. 9), employed the first-principles pseudopotential plane-wave (PPPW) total energy method. In this work on Be_2C, which was part of a study of six IIa-IV antifluorites, the only comparison of the theoretical results with experimental data was for the lattice constant. No comparison with the measured energy-loss spectra was attempted.

Here, we present a first-principles study of the ground state total energy properties and band structure and compare it with the available experimental data. To compare it with the measured low-loss spectrum, we have computed the energy-loss function $-\mathrm{Im}(1/\epsilon)$. This requires the calculation of the complex dielectric function. We have carried out the calculation for the energy region corresponding to the interband transitions between the valence and low-lying conduction bands, but not for the high-energy region. Since the low momentum exchange K-shell ELNES can be shown to be proportional to the p-wave partial density of states (PDOS) associated with the appropriate constituent,[7] we have calculated the p-wave Be and C PDOS.

The organization of this paper is as follows. In Sec. II, we briefly discuss the antifluorite crystal structure. The calculational method employed follows in Sec. III and

results are presented in Sec. IV. Conclusions are given in Sec. V.

II. STRUCTURE

Beryllium carbide crystallizes in the cubic antifluorite structure, which is the same as the calcium fluorite structure, but with the anion and cation interchanged. It has a room temperature lattice constant[10] $a = 4.342$ Å. The Be atoms are tetrahedrally and C atoms octahedrally coordinated. Figure 2 of Ref. 7 provides pictures of the cubic cell for Be_2C and of the local bonding at the Be and C atoms. The antifluorite structure is closely related to the diamond structure in the sense that one of the carbon sublattices [at $(1/4, 1/4, 1/4)$] is changed into Be and is accompanied by another Be in the opposing tetrahedral interstitial site $[(-1/4, -1/4, -1/4)]$. One may thus refer to the antifluorite structure as a filled tetrahedral structure. Wood and Zunger[11] gave a detailed discussion on the relations between the properties of Si and Mg_2Si—which are structurally equivalent to diamond and Be_2C—based on this point of view. We note that such a description occurs naturally in our computational method because we describe the diamond structure using empty spheres on the tetrahedral interstices. The perturbation from diamond to Be_2C thus consists in changing one C into Be and one empty sphere into Be.

III. CALCULATION METHOD

The calculations are carried out within the framework of density functional theory using the linear-muffin-tin-orbital (LMTO) method both in the atomic sphere approximation (ASA) with the inclusion of the so-called combined correction[12] and in the full-potential version (FP) developed by Methfessel.[13] The local-density approximation (LDA) was used for the exchange-correlation functional, which was represented by the Hedin-Lundqvist expression.[14] As usual, in treatments of open structures with the LMTO method, empty spheres were employed in the tetrahedral interstitial sites.[15] The Brillouin zone integrations, during self-consistent iterations were performed with ten Chadi-Cohen special points.[16] In the full-potential calculations, a triple κ basis set, centered on the atomic sites and including up to d waves for the first two κ values and up to p waves for the last one, was used. The κ^2 values determine the decay of the basis functions and were chosen to be -0.01, -1.00, and -2.3 Ry. This basis set was found previously to be well converged in similar tetrahedrally bonded systems.[13,17] The ASA calculations included the standard *spd* basis set on atomic and empty spheres.

To obtain the energy-loss function it is necessary to calculate the real $(\epsilon_1(\omega))$ and imaginary $(\epsilon_2(\omega))$ parts of the complex dielectric function $\epsilon(\omega)$. We compute $\epsilon(\omega)$ in the random phase approximation using a muffin-tin-orbital basis set as previously described by Alouani.[18] This calculation was carried within the ASA and used the tetrahedron method[19] for the Brillouin zone integration including a total of 525 k points in the irreducible part of the Brillouin zone. The imaginary part of the dielectric function is obtained by integrating over all vertical transitions weighted by the corresponding dipole matrix elements, which are evaluated using the one-center partial wave expansion of the wave functions. The real part is obtained by Kramers-Kronig transformation. The conduction bands were included up to about 30 eV above the valence band maximum.

IV. RESULTS

A. Energetic properties and band structure

Table I presents the ASA and FP results of our study of the energetics of our system, which were obtained by calculating the total energy for a range of lattice constant a. From a fit of those energies to the Rose *et al.*[20] expression for $E(a)$, we determined the equilibrium lattice constant a_0, the bulk modulus B and its pressure derivative B'. The cohesive energy $E_{\rm coh}$ was obtained using spin-polarized atomic calculations. Also tabulated are the values for a_0 and B reported by CC (Ref. 9) and the available experimental values.[10,21,22]

The first thing we note is the closeness of the ASA and FP results. Aside from the pressure derivative of the bulk modulus, which is essentially a higher elastic constant, the results differ by less than a few percent. We note that the calculated a_0 is only about 1% lower than the measured room temperature value and about 1 % higher than the value computed by CC.[9] Our value is quite satisfactory particularly when one notes that an estimated correction for thermal expansion will reduce the discrepancy by roughly a half. To our knowledge, there

TABLE I. Energetic properties of Be_2C.

	FP	ASA	PPPW[a]	Expt.
Lattice constant a (Å)	4.27	4.29	4.23	4.34[b]
Bulk modulus B (GPa)	216	213	216	
Pressure derivative of the bulk modulus dB/dp	3.5	4.18		
Cohesive energy (eV/atom)	5.86	6.03		5.08[c]

[a]Corkill and Cohen (Ref. 9).
[b]Wyckoff (Ref. 10).
[c]Using formation energy from CRC Handbook (Ref. 21) and cohesive energies of the elements from Gschneider (Ref. 22).

is no direct data on B. However, the report by Coobs and Koshuba[23] that Be_2C is slightly harder than SiC whose $B = 233$ GPa, along with the rough correlation of hardness and bulk modulus, suggests that the calculated value of B is quite reasonable. The present value is the same as that found in CC.[9] The cohesive energy is 15–18 % overestimated as is usual for the LDA. This is known to be mostly due to the relative inaccuracy of LDA for the free atoms.

Figure 1 displays the band structure obtained by the FP method. The bands calculated by the ASA method are almost identical to those in Fig. 1 and hence are not reproduced. Table II lists the values of a number of band widths, the ionic and principal band gaps, and a few other energy differences given by the two calculations. Also included are the corresponding values reported in HR (Ref. 8) and CC.[9] The largest discrepancy between the ASA and FP band-structure results is only 0.2 eV. We note that the accuracy of the ASA results is not surprising in view of the symmetry of the calcium fluorite structure.

The present results are found to be in quite good agreement with those of CC.[9] The largest discrepancy between the two sets of bands over the fairly wide energy range covered in Fig. 1 is about 0.4 eV.

With respect to the other two band-structure calculations, our results are more similar to the APW than to the semiempirical tight-binding results. While the ordering of the states in HR is the same as in the present work, there are significant quantitative differences. Perhaps, the most significant of these is the magnitude of the principal band gap, which is indirect ($\Gamma_{15} - X_1$). We find it to be 1.21 eV, while HR find the appreciably larger value of 2.98 eV.

The band structure of Disko *et al.*, on the other hand, differs both qualitatively and quantitatively from the present and the other first-principles band structures. Their conduction band minimum occurs at L instead of X; and the value for their indirect gap ($\Gamma_{15} - L_{2'}$) is roughly 4 eV.

The origin of the appreciable quantitative differences

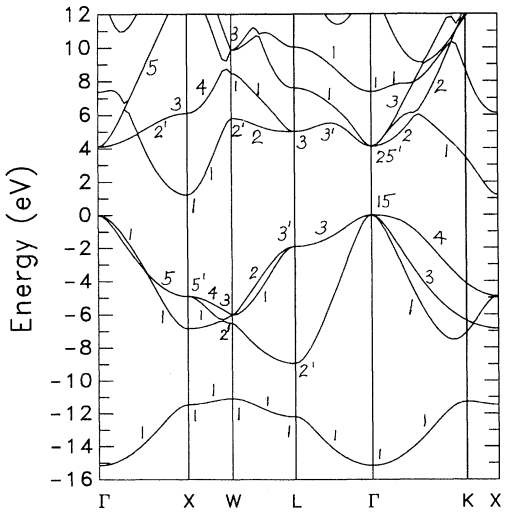

FIG. 1. Electronic band structure of Be_2C.

TABLE II. Band widths and band gaps for Be_2C (in eV).

		FP	ASA	APW [a]	PPPW [b]
Band widths	$\Gamma_1 - W_1$	4.05	4.0	3.1	4.26
	$L_{2'} - \Gamma_{15}$	8.94	9.0	7.2	9.16
Band gap	$W_1 - L_{2'}$	2.16	2.2	3.5	2.06
	$\Gamma_{15} - X_1$	1.21	1.15	3.0	1.23

[a]Herzig and Redinger (Ref. 8).
[b]Corkill and Cohen (Ref. 9).

between the HR's and present band structure deserves some further scrutiny. We note that both our and HR's calculations used the Hedin-Lundqvuist[14] exchange and correlation parametrization. Our calculations included scalar-relativistic effects and was performed at the theoretical equilibrium lattice constant of $a = 4.29$ Å; theirs was nonrelativistic and used the experimental lattice constant of $a = 4.342$ Å. However, neither of these two differences can come close to explaining the discrepancies noted above. We found that neglecting the relativistic effects increased the gap by only 0.02 eV (a small shift, as expected for these light elements); and, with an estimated deformation potential of about 1 eV, our slight underestimate of the lattice constant only changes the gap by about 0.1 eV from the value obtained at the experimental lattice constant. We, thus, conclude that the difference in band structure between our and HR's calculation is probably due either to their use of the muffin-tin approximation—which, as suggested above, is of questionable accuracy—or to an inadequate convergence of their plane-wave basis set. The FP calculations, of course, do not make any approximations regarding the shape of the potential.

Calculations using the atomic sphere approximation are more accurate than those using muffin-tin potentials especially when the combined correction is included. Also relevant in this connection is our use of empty spheres, which allows for a more accurate treatment of the interstitial regions. The adequacy of the LMTO basis set with s, p, and d partial waves centered on the atoms and on empty spheres for systems of fluorite (or anti-fluorite) structure has been amply demonstrated in previous calculations for $NiSi_2$ and $CoSi_2$ (Ref. 24) and in many other calculations.

Finally, we recall the well-known fact that the LDA underestimates the low-energy excitation spectra, e.g., the band gap. Thus, a comparison of the band structure to empirical excitation data should require a shift of the LDA conduction band states upwards by some presently undetermined amount. The gap correction in another closely related low Z material, c-BN, is 2.1 eV.[25] Our analysis of the electron-energy-loss spectrum in subsection C will allow us to determine an experimental correction to the gap of 2 eV.

B. Partial densities of states and ELNES spectra

The C and Be K-edge electron-loss-near-edge-spectroscopy (ELNES) measurements reported by Disko *et al.*[7] constitute a major share of the experimental data

relating to the electronic structure of Be_2C. Disko *et al.* show that the small momentum transfer loss spectra is approximately proportional to the p-like partial density of states (PDOS) in the conduction band. Figure 2 presents unbroadened C and Be PDOS for the valence and low-lying conduction bands. It can be seen that the Be PDOS tends to be larger than the C-PDOS for the conduction bands, while the opposite is true for the valence bands. This is consistent with both CC's and HR's results and also with the ELNES data. Figure 3 displays the p DOS convoluted with a Gaussian broadening function with a width of 2.5 eV.

Since there is considerable uncertainty in the core level positions, it is necessary to shift the ELNES spectra in order to effect a comparison with the PDOS. We align the spectra so that the first peaks of the Be- and the C-ELNES spectra (labeled a and 1, respectively) coincide with the first peaks of the corresponding PDOS. The peaks in the PDOS, which occur at ~ 6.5 eV above the valence band maximum, come from the lowest conduction band in the region of the BZ near L, where the bands are quite flat. (We note that those are even flatter in HR's results leading to more pronounced first peaks than ours, particularly for C.) The above alignment, which differs from that made by Disko *et al.*, appears to us to be the most physically plausible one. The magnitudes of the ELNES curves, which are indicated by the thicker curves, have been adjusted. This has required a relative increase in the magnitude for C data (see below).

The issues of peak positions, relative magnitude and spectral shapes are clearly intertwined. We start with the positions. The Be d and the C 2 peaks, which are relatively strong in the data, and the pronounced dip at about 18 eV in the C spectrum are the ones for which a comparison between theory and experiment is most unambiguous. As can be seen in Fig. 3, these positions agree to within 1 eV. The positions of the Be b and c peaks and the C 3 peak, which are weaker and significantly effected by overlap, can be located but only with a larger uncertainty, about 2 eV. The positions of the corresponding peaks in the PDOS agree with those in the data within the estimated uncertainty. While the shape

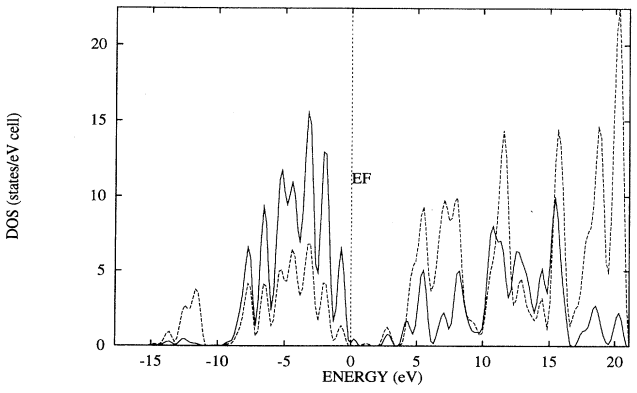

FIG. 2. Unbroadened p-wave partial densities of states for Be_2C. The solid curve is for C and the dashed curve for Be.

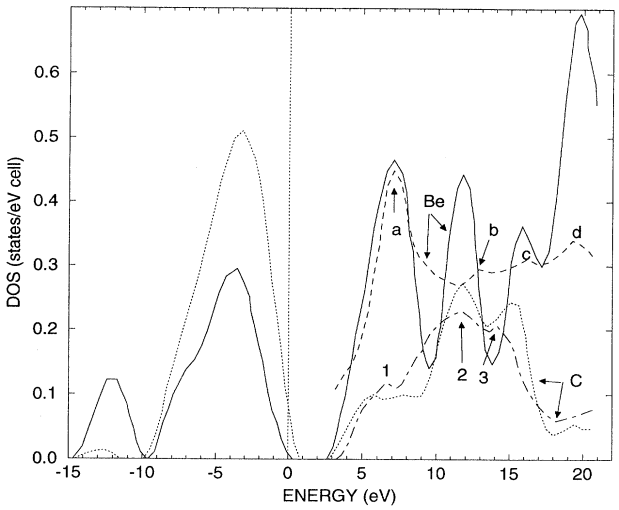

FIG. 3. Broadened p-wave partial densities of states (PDOS) and measured K-shell electron-energy-loss-near-edge fine structure (ELNES) for Be and C. The thin solid (dashed) curve is the PDOS for Be (C) and the thick curves are the measured ELNES spectra.

of the C PDOS is in reasonable accord with the data, the relative magnitude of the Be b, c, and d PDOS peaks are considerably larger than in the data. This aspect of the comparison is complicated principally by the omission in the PDOS of the energy dependencies of the matrix elements (squared) and of the linewidth. An increase in the widths with energy, which is to be expected, would tend to partially "wash out" the moderately high-energy Be b, c, and C 3 features. The square of the dipole matrix element, which is proportional to the oscillator strength, is expected to decrease with increasing energy as is the case in the optical transitions in the visible and near UV regions. In fact, the f-sum rule requires a decrease. For the present problem, the effect should be pronounced for as the final state spreads out in the cell with increasing energy, its overlap with the highly localized $1s$ state should decrease significantly. The substantial effect of these two factors can be appreciated by a comparison of the d peaks in the PDOS and in the measurements.

Another aspect of the comparison worth noting is the fact that the C-ELNES curve of Ref. 7 was—as mentioned earlier—multiplied by an additional factor of about 3 over that for the Be ELNES to obtain the curves plotted in Fig. 3. When the differences in the Be and C PDOS are taken into account, this implies that the squared matrix element for Be is approximately three times that for C. We attribute this to the fact that the C-$1s$ state is considerably more tightly bound than the Be-$1s$ state.

Our interpretation of the ELNES data differs markedly from the tight-binding results of Disko *et al.*, who, in their alignment of the two loss spectra, place the onset of the spectrum for C about 5 eV (9 eV for the peak 1) above the onset for Be. Their argument for doing that is based on their assertion that the C p-PDOS for the conduction band is essentially negligible until about 10

eV above the conduction band minimum. As is evident in Fig. 3, while the p-PDOS for C is smaller than that for Be (by roughly a factor of 3), it is not negligible and, furthermore, does not turn on abruptly at some energy above the conduction band edges.

We note that the multiple scattering calculations of the ELNES spectra in Disko *et al.*[7] provide a better agreement in line shape with the measured spectra. Since this calculation included matrix element effects, it confirms the importance of the latter for the line shape. In agreement with our conclusions, no need is found to include excitonic final-state effects between the core-hole and the excited conduction electron.

C. Dielectric functions and the low-energy-electron-loss spectrum

The other spectral function reported by Disko *et al.*[7] that bears on the electronic structure is the energy electron loss in the low-loss region. That function is given by $-\mathrm{Im}(1/\epsilon(\omega))$, where $\epsilon(\omega)$ is the complex dielectric function mentioned in Sec. III. The $\epsilon(\omega)$ depends on the excitation, or quasiparticle, spectrum. As we noted in subsection A above, the LDA underestimates the true band gap by a significant amount, which is generally referred to as the self-energy or gap correction. In studies of several semiconducting systems,[26–28,5] it was found that a single overall upwards shift (or, correction) to all of the relevant low-lying conduction bands lead to $\epsilon(\omega)$, which provided satisfactory descriptions of the optical properties of those materials. In those systems, the band gaps were known empirically and hence the corrections were obtained directly and trivially. Since the empirical gap is not known for Be_2C, another approach is necessary. Here, we adjust the shift so that the peak in $-\mathrm{Im}(1/\epsilon(\omega))$ coincides with the peak of the measured spectrum. The shift is 2 eV. This appears to be reasonable in light of corrections for the other semiconductors.

Figure 4 shows the real and imaginary parts of the dielectric function—with the shift included—over a 20 eV range. As is well known, all of the optical properties—the reflectance and absorbance—of this compound can be obtained in terms of these two functions. At present, the relevant data do not exist.

In Fig. 5, we display the band-to-band decomposition of $\epsilon_2(\omega)$. From this figure and an examination of a plot of interband energies throughout the BZ, one can identify the bands and regions of $\vec{k}$ contributing to the structure in $\epsilon_2(\omega)$ and $\epsilon_1(\omega)$. For example, the fairly weak structures at 8.3 eV and 9.2 eV are associated with transition between the upper valence band and the two lowest conduction bands around the points X and L, respectively. The main peak at 9.8 eV comes from regions of parallel bands along the Σ axis near K, with some contribution from nearly parallel bands along the Δ axis about 0.4 of the distance between Γ and X.

The measured and calculated loss functions are shown in Fig. 6. A small constant background subtraction (the value of the data in the region between the forward peak and the apparent onset) was applied to the data. The

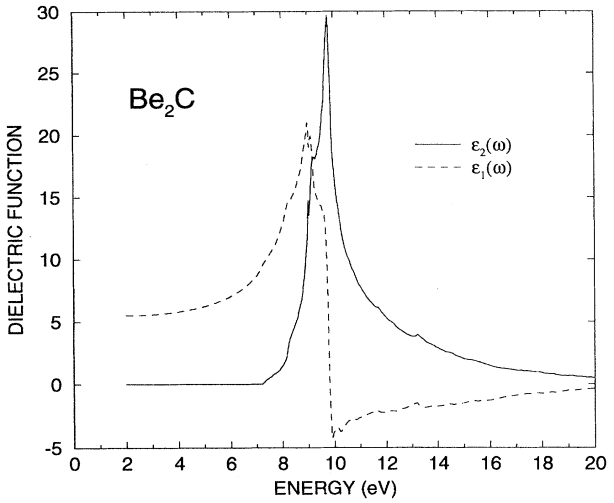

FIG. 4. The real (ϵ_1) and imaginary (ϵ_2) parts of the dielectric function for Be_2C. The effects of a rigid upwards shift of 2.0 eV of the conduction bands are included.

original $-\mathrm{Im}\epsilon^{-1}(\omega)$ function was subjected to a constant 1.0 eV Gaussian broadening. The peak of the calculated curve was aligned with that of the measured function, which is at the plasma energy of 22.7 eV, by the 2.0 eV shift to higher energies mentioned above. The plasma energy associated with the Be_2C valence electrons is calculated to be 22.7 eV, which is in excellent agreement with the peak position in the data. It can be seen that the shape of the calculated loss function generally matches that of the data satisfactorily. The fit is particularly good over the whole of the lower half of the curves, from the onset to peak. The major discrepancy occurs in the relatively high-energy region of 25 to 30 eV, where the calculations fall well below the measurements. This could

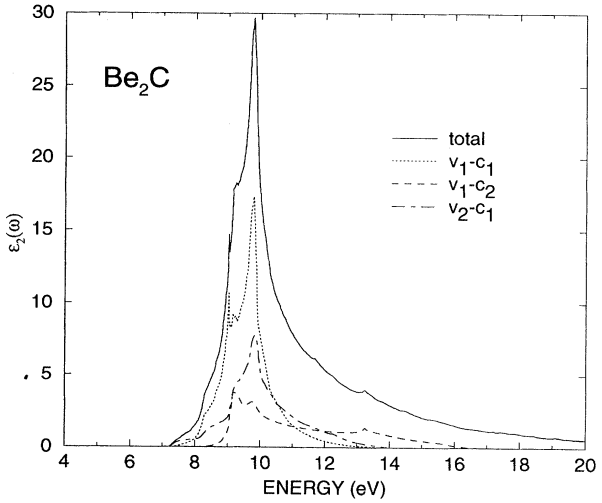

FIG. 5. The decomposition of the imaginary part of the dielectric function into band-to-band contributions. The two highest valence (lowest conduction) bands are labeled v_1 and v_2 (c_1 and c_2).

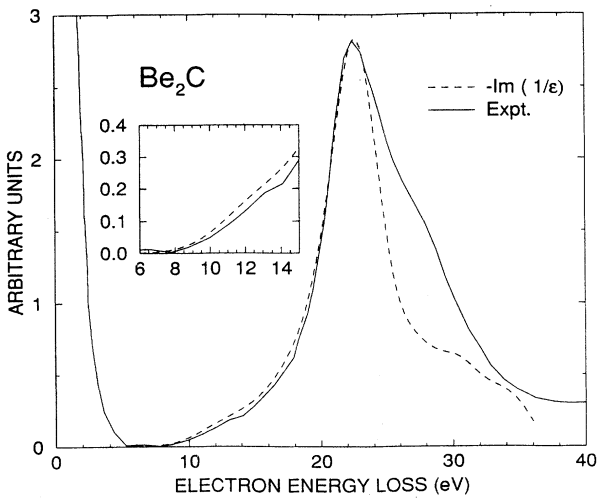

FIG. 6. Calculated and measured electron energy loss. A broadening of 1 eV is included in the calculated spectrum. The ordinate is in dimensionless units for $-\mathrm{Im}(1/\epsilon)$ and arbitrarily scaled intensity units for the experiment.

be due to an increasing linewidth at higher energies, as discussed earlier. In part, it could also be due to the involvement of bands lying relatively far above the center of the linearization panel.

It is also of interest to examine the two loss functions in the regions of their "onsets." An expanded picture of this region appears in the inset. There it can be seen that the apparent onset in the data at about 8.0 eV is well reproduced in the calculations. That contribution corresponds to the broadened structures in ϵ_2 at about 8.5 eV. This agreement provides additional evidence of the accuracy of the present band structure when the self-energy correction is incorporated.

D. The bonding

Finally, we discuss the nature of the bonding. Herzig and Redinger[8] concluded that the bonding was quite ionic on the basis of the charge distribution per sphere. Corkill and Cohen reached the same conclusions from their charge density plots. Clearly, the details of the analysis depends on the way the unit cell is partitioned—more practically, on the choice of the radii of the spheres within which the charge is computed. Because of our use of equal sphere radii while HR had smaller spheres around the Be than around the C atoms, we find slightly smaller charge differences between C and Be than they do, as can be seen in Table III. A different and perhaps less ambiguous way of portraying the ionicity is to consider the relative positions of the center of the band potential parameters C_{Rl} as defined in Ref. 12. The latter are also given in Table III. We can see that the Be_l band centers lie significantly above the corresponding C_l band centers. This clearly indicates that the bonding has a significant ionic character with charge transfer from the Be to the C atoms. We thus agree with HR's conclusion,[8] but on a somewhat different basis.

TABLE III. Charge distribution and band center parameters for Be_2C.

	Present	Ref. 8
q_{Be_s}	1.26	1.31
q_{Be_p}	0.43	0.41
q_{C_s}	2.90	3.04
q_{C_p}	0.91	0.88
C_{Be_s} (eV)	0.03	
C_{C_s} (eV)	-0.95	
C_{Be_p} (eV)	0.85	
C_{C_p} (eV)	0.16	

V. CONCLUSIONS

First-principles studies of the electronic structure and energetic properties of Be_2C are carried out by the LMTO method in both the ASA and full potential versions. The results from the two approaches are, as expected, in very good agreement. The band structures are also compared with the two previous calculations of this material. The calculated lattice constant is in good agreement with the measured value. The bulk modulus is found to be fairly high, 216 GPa, which is consistent with the fact that the material is known to be about as hard as SiC. The complex dielectric reponse function is also calculated, and from it the energy-loss spectrum in the low-loss region is obtained. This is found to be in good agreement with the measured loss function especially when a rigid 2 eV shift (corresponding to the LDA self-energy correction to the band gap) is applied to the conduction bands. A comparison is made between the measured Be and C K-shell ELNES and the calculated Be and C p state partial density of states, which should be proportional to the ELNES for small momentum transfer. Good agreement is found. This agreement along with that for the loss spectrum in the low-energy region tends to confirm the accuracy of the present band structure. The band gap is found to be indirect with the valence band maximum at Γ and conduction band minimum at X and to have the relatively low LDA value of 1.2 eV. When combined with the gap correction, the quasiparticle gap should be about 3 eV.

ACKNOWLEDGMENTS

We thank M. Alouani for providing us the dielectric function program. The work was supported by NSF-MRG Grant No. DMR-89-03527. One of us (C. H. Lee) thanks the encouragement from Professor C. I. Um and the support from Korea Science and Engineering Foundation (KOSEF). Calculations were done using facilities of the Ohio Supercomputer Center.

* Present address: Department of Physics, Korea University, Seoul 136-701, Korea.

[1] See, for example, *Diamond, Silicon Carbide and Related Wide Bandgap Semiconductors*, edited by J. T. Glass, R. Messier, and N. Fujimori, MRS Symposia Proceedings No. 162 (Material Research Society, Pittsburgh, 1990).

[2] A. Argoitia, J. C. Angus, L. Wang, X. I. Ning, and P. Pirouz, J. Appl. Phys. **73**, 4315 (1993).

[3] W. R. L. Lambrecht and B. Segall, J. Mater. Res. **7**, 696 (1992).

[4] W. R. L. Lambrecht and B. Segall, Phys. Rev. B **45**, 1485 (1992).

[5] W. R. L. Lambrecht, C. H. Lee, K. Kim, A. G. Petukhov, E. A. Albanesi, and B. Segall, in *Proceedings of NATO Advanced Workshop on Wide-Bandgap Electronic Materials, Minsk, May 4–6, 1994*, Vol. 106 of *NATO Advanced Study Institute, Series B: Physics*, edited by M. Prelas, P. Gielisse, and V. Varichenko (Kluwer, Dordrecht, The Netherlands, 1995).

[6] A. G. Petukhov, W. R. L. Lambrecht, and B. Segall, Phys. Rev. B **49**, 4549 (1994).

[7] M. M. Disko, J. C. H. Spence, O. F. Sankey, and D. Saldin, Phys. Rev. B **33**, 5642 (1986).

[8] P. Herzig and J. Redinger, J. Chem. Phys. **82**, 1 (1985).

[9] J. L. Corkill and M. L. Cohen, Phys. Rev. B **48**, 17 138 (1993).

[10] R. W. G. Wyckoff, *Crystal Structures*, 2nd. ed. (Interscience, New York, 1963), Vol. 1, p. 241.

[11] D. M. Wood and A. Zunger, Phys. Rev. B **34**, 4105 (1986).

[12] O. K. Andersen, Phys. Rev. B **12**, 3060 (1975). H. L. Skriver, *The LMTO Method* (Springer, New York, 1984); O. K. Andersen, O. Jepsen, and M. Šob, in *Electronic Band Structure and its Applications*, edited by M. Yussouf (Springer, Heidelberg, 1987), p. 1.

[13] M. Methfessel, Phys. Rev. B **38**, 1537 (1988); M. Methfessel, C. O. Rodriguez, and O. K. Andersen, *ibid.* **40**, 2009 (1989).

[14] L. Hedin and B. I. Lundqvist, J. Phys. C **4**, 2064 (1971).

[15] D. Glötzel, B. Segall, and O. K. Anderson, Solid State Commun. **36**, 403 (1980).

[16] D. J. Chadi and M. L. Cohen, Phys. Rev. B **7**, 692 (1973); **8**, 5747 (1973).

[17] W. R. L. Lambrecht, B. Segall, M. Methfessel, and M. van Schilfgaarde, Phys. Rev. B **44**, 3685 (1991).

[18] M. Alouani, L. Brey, and N. E. Christensen, Phys. Rev. B **37**, 1167 (1988).

[19] O. Jepsen and O. K. Andersen, Solid State Commun. **9**, 1763 (1971).

[20] J. H. Rose, J. R. Smith, F. Guinea, and J. Ferrante, Phys. Rev. B **29**, 2963 (1984).

[21] *CRC Handbook of Chemistry and Physics*, 68th ed., edited by R. C. Weast (CRC Press, Boca Raton, 1988).

[22] K. A. Gschneider, Jr., in *Solid State Physics, Advances in Research and Applications*, edited by F. Seitz and D. Turnbull (Academic Press, New York, 1964), Vol. 16, p. 275.

[23] J. H. Coobs and W. J. Koshuba, J. Electrochem. Soc. **99**, 115 (1952).

[24] W. R. L. Lambrecht, N. E. Christensen, and P. Blöchl, Phys. Rev. B **36**, 2493 (1987).

[25] W. R. L. Lambrecht and B. Segall, Phys. Rev. B **47**, 9289 (1993).

[26] W. R. L. Lambrecht, B. Segall, W. Suttrop, M. Yoganathan, R. P. Devaty, W. J. Choyke, J. A. Edmond, J. A. Powell, and M. Alouani, Appl. Phys. Lett. **63**, 2747 (1993).

[27] W. R. L. Lambrecht, B. Segall, M. Yoganathan, W. Suttrop, R. P. Devaty, W. J. Choyke, J. A. Edmond, J. A. Powell, and M. Alouani, Phys. Rev. B **50**, 10 722 (1994).

[28] W. R. L. Lambrecht, in *Diamond, SiC and Nitride Wide-Bandgap Semiconductors*, edited by C. H. Carter, Jr., G. Gildenblat, S. Nakamura, and R. J. Nemanich, MRS Symposia Proceedings No. 339 (Material Reserch Society, Pittsburgh, 1994) p. 565.